

ATP2C1 knockdown induces abnormal expressions of cytoskeletal and tight junction proteins mimicking Hailey–Hailey disease

Mingzhu Zhou, Shiran Kang, Yumin Xia, Dingwei Zhang, Wenwen Chen¹

Department of Dermatology, The Second Affiliated Hospital of Xi'an Jiaotong University, Xi'an, ¹Department of Dermatology, Yangling Demonstration Zone Hospital, Yangling, China

Abstract

Background: Hailey–Hailey disease (HHD) is a rare, autosomal dominant, hereditary skin disorder characterised by epidermal acantholysis. The HHD-associated gene ATPase calcium-transporting type 2C member 1 (*ATP2C1*) encodes the protein secretory pathway Ca^{2+} ATPase1 (SPCA1), playing a critical role in HHD pathogenesis.

Aims: We aimed to investigate the effect of *ATP2C1* knockdown on keratinocytes that mimicked acantholysis in HHD.

Methods: Immunohistochemistry (IHC) was employed to evaluate the levels of cytoskeletal and tight junction proteins such as SPCA1, P-cofilin, F-actin, claudins, occludin, and zonula occludens 1 in the skin biopsies of patients with HHD. Subsequently, the expression of these proteins in cultured *ATP2C1* knockdown keratinocytes was analysed using Western blotting and immunofluorescence. Furthermore, we assessed the proliferation, apoptosis, and intracellular Ca^{2+} concentrations in the *ATP2C1*-knocked keratinocytes.

Results: The results showed decreased levels of these proteins (SPCA1, P-cofilin, F-actin, claudins, occluding, and zonula occludens 1) in HHD skin lesions. Moreover, their levels decreased in human keratinocytes transfected with *ATP2C1* short hairpin RNA, accompanied by morphological acantholysis. Furthermore, the proliferation and apoptosis of the keratinocytes, as well as intracellular calcium concentrations in these cells, were not affected.

Limitations: The limitations of this study are the absence of animal experiments and the failure to explore the relationship between skeletal and tight junction proteins.

Conclusion: The present study indicated that *ATP2C1* inhibition led to abnormal levels of the cytoskeletal and tight junction proteins in the keratinocytes. Therefore, keratinocytes can mimic HHD-like acantholysis and serve as an *in vitro* model, helping develop treatment strategies against HHD.

Key words: *ATP2C1*; F-actin; Hailey–Hailey disease; P-cofilin; SPCA1

Introduction

Hailey–Hailey disease (HHD) or familial benign chronic pemphigus, an uncommon, autosomal dominant genodermatosis with complete penetrance is characterised by flaccid vesicles and blisters, with a predilection for intertriginous regions, such as the retroauricular folds,

axillae, lateral aspects of the neck, and inguinal and perianal regions.¹ A genetic defect in the Adenosine Triphosphatase (ATP) calcium-transporting type 2C member 1 gene (*ATP2C1*) located on chromosome 3q21-q24 causes this disease.² *ATP2C1* encodes a protein named human secretory pathway $\text{Ca}^{2+}/\text{Mn}^{2+}$ -ATPase pump type 1 (SPCA1), which is

How to cite this article: Zhou M, Kang S, Xia Y, Zhang D, Chen W. ATP2C1 knockdown induces abnormal expressions of cytoskeletal and tight junction proteins mimicking Hailey–Hailey disease. Indian J Dermatol Venereol Leprol. doi: 10.25259/IJDVL_853_2023

Corresponding author: Dr. Wenwen Chen, Department of Dermatology, Yangling Demonstration Zone Hospital, Yangling, China. 15736875920@163.com

Received: August, 2023 **Accepted:** October, 2023 **Epub Ahead of Print:** May, 2024

DOI: 10.25259/IJDVL_853_2023 **Supplementary files available on:** https://doi.org/10.25259/IJDVL_853_2023

This is an open-access article distributed under the terms of the Creative Commons Attribution-Non Commercial-Share Alike 4.0 License, which allows others to remix, tweak, and build upon the work non-commercially, as long as the author is credited and the new creations are licensed under the identical terms.

present in the Golgi apparatus membrane and plays a role in $\text{Ca}^{2+}/\text{Mn}^{2+}$ transportation, maintaining a balance between Ca^{2+} concentration in the cytoplasm and Golgi apparatus.³ A hereditary mutation in *ATP2C1* results in insufficient SPCA1 levels, leading to a reduction in $\text{Ca}^{2+}/\text{Mn}^{2+}$ concentrations in the Golgi apparatus. This alteration disrupts the functions of Golgi apparatus proteins that depend on normal Ca^{2+} levels, causing abnormalities in intercellular connections in keratinocytes and ultimately leading to desquamation in the skin epidermis.

Despite knowing that *ATP2C1* mutations are the primary cause of HHD, the precise molecular mechanism of the gene in HHD has not been elucidated. The widespread desquamation of spinous-layer cells in HHD is probably associated with the levels of tight junction proteins and desmosomes. In a study, an *in vitro* cell model was established by *ATP2C1* transfection, and its knockdown showed that the levels of desmosomes remained unchanged. In contrast, the levels of the tight junction protein claudin increased, and those of zonula occludens protein 1 (ZO-1) decreased.⁴ Therefore, we shifted our focus from desmosomes to exploring the link between HHD and tight junction proteins. ZO-1 directly interacts with occludin, claudin 1, and claudin 4 via the post-synaptic density disc large Zo-1 domains. In contrast, its C-terminus directly binds to F-actin to interact with the F-actin cytoskeleton.^{5,6} The actin-severing protein cofilin binds to the phosphorylated region of SPCA1. It gets phosphorylated to form P-cofilin, which, in turn, interacts with F-actin, resulting in SPCA1 activation and Ca^{2+} and Mn^{2+} pumping into the Golgi apparatus lumen under adequate ATP supply.⁷ Moreover, epithelial cells participate in cell adhesion and tight junction protein connections with the help of Ca^{2+} and F-actin polymerisation.⁸ Therefore, we hypothesised an association between HHD occurrence and P-cofilin and F-actin levels.

Moreover, we performed this study to evaluate the relationship between the levels of SPCA1 and cytoskeletal or tight junction proteins in HHD skin lesions. Furthermore, the effect of *ATP2C1* knockdown on these protein levels and morphological acantholysis was analysed using keratinocytes.

Materials and Methods

Human tissue samples

HHD skin samples were obtained from patients (n = 22) with HHD after examining their clinical features and histopathology. Normal skin tissues were collected from healthy donors (n = 20) undergoing plastic surgery. For keratinocyte experiments, human foreskin tissues were isolated from healthy patients who underwent circumcision. This study was performed under the guidance and supervision of the Hospital Research Ethics Committee, and written informed consent was obtained from all subjects.

Immunohistochemistry (IHC)

As described previously,⁹ tissues were cut into 5- μm paraffin sections. The sections were subjected to dewaxing

treatment, followed by antigen retrieval with sodium citrate. After incubation with 2% goat serum (Beyotime Biotech, Shanghai, China), the samples were incubated with primary antibodies at 4°C overnight. These primary antibodies were mouse antibodies against SPCA1 (Proteintech, Rosemont, Illinois, USA), F-actin (Abcam, Cambridge, MA, USA) and rabbit antibodies against glyceraldehyde-3-phosphate dehydrogenase (GAPDH; Proteintech), occludin (Abcam), claudin 1 (Abcam), claudin 4 (Abcam), ZO-1 (Abcam), and P-cofilin (Cell Signaling Technology, Danvers, MA, USA). Then, the sections were incubated with a horseradish peroxidase-labelled goat anti-Rabbit/Mouse antibody (DAKO, Glostrup, Denmark) and the 3, 3'-diaminobenzidine chromogen substrate (DAKO). Phosphate-buffered saline controls were used for all samples.

Cell culture and short hairpin RNA (shRNA) transfection

Keratinocytes were obtained as described previously,¹⁰ and cultured in the keratinocyte serum-free medium (KFSM) with low Ca^{2+} (0.09 mM; KFSM; Sciencell, San Diego, CA, USA). The cultured cells at passage 2 or 3 were divided into blank, control shRNA, and *ATP2C1* shRNA lentivirus transfection groups and seeded on 6-well plates. A total of 20 μl of shRNA lentivirus (5×10^7 TU/mL) and enhancement solutions (Genechem, Shanghai, China) were added to the culture medium of the *ATP2C1* shRNA group. The exact amounts of the harmful virus and enhancement solution were added to the control shRNA group. After 8 h of transfection, the medium was replaced with regular KFSM. After culturing for 72 h, the keratinocytes were further cultured in the KFSM containing 1 $\mu\text{g}/\text{mL}$ puromycin for cell selection. When the blank-group cells were completely killed by puromycin, and no more cells died in the *ATP2C1* shRNA group, the surviving cells were used for further experiments.

Quantitative reverse transcriptase polymerase chain reaction (qRT-PCR)

Total RNA was extracted from fresh tissues and cell cultures using the Trizol reagent (Invitrogen, Carlsbad, CA, USA). RNA was reverse transcribed into complementary DNA (cDNA) using a commercial cDNA kit (Takara Bio, Shiga, Japan). Then, qPCR was performed on a 7900HT Fast PCR System (Applied Biosystems, Waltham, MA, USA). SYBR Green Master Mix (Takara Bio, Shiga, Japan) was a fluorescent dye. The synthesis of all target gene primers was performed by Bioscience (Shanghai, China) using *GAPDH* primers as internal references. The primer sequences are listed in Supplementary Table 1.

Cellular immunofluorescence

The cells were cultured in glass-bottom culture dishes (MatTek, Ashland, MA, USA) and fixed with the 4% paraformaldehyde (PFA) solution. The cells were permeabilised using Triton and subsequently blocked using a goat serum. Then, the cells were incubated with primary antibodies (see above under (IHC)) at 4°C overnight. Subsequently,

AL488-labelled goat anti-rabbit/mouse IgG (Beyotime, Shanghai, China) was added for staining. After incubating with the 4',6-diamidino-2-phenylindole (DAPI) solution (Het Biotech, Xi'an, China), the cells were observed under a digital confocal microscope (Leica, Wetzlar, Germany).

Western blotting technique

Protein lysates were prepared from the cell cultures using the radioimmunoprecipitation buffer (Het Biotech). Protein concentrations were determined using the Bicinchoninic Acid Protein Assay Kit (Het Biotech). The samples were separated on electrophoresis gels, followed by transfer onto polyvinylidene difluoride membranes (Millipore, Burlington, MA, USA). Horseradish peroxidase goat anti-rabbit/mouse immunoglobulin G (1 µg/ml; Abcam) was used as a secondary antibody. Then, an electrochemiluminescence kit (Millipore) was used for signal detection. The intensities of all protein bands were compared with the intensities of Glyceraldehyde-3-phosphate dehydrogenase (GAPDH) bands of the same filter. The obtained band intensities were quantified using the ImageJ software (National Institutes of Health, Bethesda, MD, USA).

Transmission electron microscopy (TEM)

The cells were fixed using the electron-microscopy-specific fixative, followed by neutral phosphate buffer-osmic acid addition. After dehydration and embedding, the cells were cut into 60–80 nm ultra-thin sections. Following double staining with 1% uranyl acetate and lead citrate, the sections were visualised, and images were captured with a transmission electron microscope (HT7700, HITACHI, Tokyo, Japan).

Cell proliferation and apoptosis

The cells were cultured in 96-well plates and transfected with shRNA. After transfecting for 24, 48, and 72 h, the cultures were analysed for cell proliferation. The cell counting kit-8 (CCK-8) solution (Beyotime) was added, and the cells were incubated at 37°C for 2 h. Absorbance was measured at 450 nm.

Cell apoptosis was determined using flow cytometry. After 48 h of transfection, the cells were diluted to 1×10^6 cells/mL, incubated with a binding buffer, and mixed with 7-amino actinomycin D (7-AAD) (red fluorescence) and annexin V-phycoerythrin (orange-red fluorescence). The data were analysed using the LSRII instrument (BD Biosciences, San Jose, CA, USA) and processed using the FlowJo7.6.1 software (BD, San Diego, CA, USA).

Intracellular Ca²⁺ detection

The cells in the three groups were transferred to black 96-well plates and cultured for 24 h. The culture medium was then replaced with an assay buffer containing fluo-3 AM (0.5 µM, Beyotime), and the cells were further incubated at 37°C for 60 min for fluorescence probe loading.¹¹ Intracellular fluo-3 fluorescence was then monitored at an excitation wavelength of 506 nm and an emission wavelength of 526 nm using

a fluorescent enzyme labelling instrument (Labsystems Multiskan MS, Finland). Relative fluorescence values compared the intracellular Ca²⁺AQ concentration of the three groups.

Statistical analysis

The experimental results were subjected to statistical analysis and graphing using the ImageJ and GraphPad Prism 8.0 software. A two-sample independent t-test was performed for comparing any two groups, and an analysis of variance was performed for comparing the three groups. Differences were considered statistically significant at $p < 0.05$.

Results

Cytoskeletal and tight junction proteins were deregulated in the skin lesions of HHD

The IHC analysis showed that the levels of SPCA1, F-actin, P-cofilin, claudin 1, claudin 4, occludin, and ZO-1 were high in the normal epidermis and low in the HHD lesions [Figures 1a and 1b]. Their quantitative analysis using ImageJ showed decreased levels of these proteins [Figure 1c].

ATP2C1 was inhibited in cultured keratinocytes by shRNA transfection

The keratinocytes exhibited morphological changes after shRNA transfection and returned to normal 96 after transfection, suggesting successful transfection (Supplementary Figure 1). The immunofluorescence analysis showed that SPCA1 levels decreased significantly in the ATP2C1 shRNA group with no difference between the two controls ($p < 0.050$) [Figure 2a]. Conformably, ATP2C1 mRNA and SPCA1 levels decreased in the ATP2C1 shRNA group [Figures 2b and 2c].

The transmission electron microscopy (TEM) results showed that the cells in the blank group exhibited no swelling. Several tight junctions were observed between the cells with narrow intercellular space. The cells in the control shRNA group showed mild swelling, with lesser intercellular tight junctions accompanied by more expansive intercellular space. The shRNA-transfected cells showed swelling with a few tight junctions and widened intercellular space [Figure 2d].

ATP2C1 knockdown suppressed P-cofilin and F-actin

We examined the levels of P-cofilin and F-actin in the cells using immunofluorescence. Compared with the blank group, the control shRNA group showed minimal changes in P-cofilin and F-actin levels. However, the shRNA-transfected cells showed significantly reduced fluorescence intensity ($p < 0.05$), accompanied by considerably decreased F-actin ring formation around the cell periphery and reduced F-actin filamentous pseudopodia between the cells [Figures 3a and 3b]. Compared with the blank and control shRNA groups, the ATP2C1 shRNA group showed lower P-cofilin mRNA transcript levels ($p < 0.050$) [Figure 3c]. Consistently, the western blotting technique results showed decreased P-cofilin and F-actin levels after shRNA transfection. ($p < 0.05$) [Figures 3d and 3e].

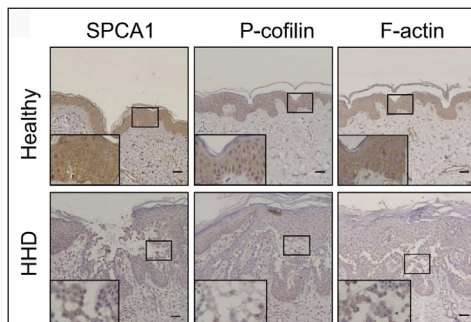


Figure 1a: SPCA1, cytoskeletal, and tight junction proteins are poorly expressed in the skin lesions of patients with HHD. Immunohistochemistry (IHC) was performed for the protein expression in the paraffin sections. SPCA1, Secretory pathway Ca^{2+}/Mn^{2+} Adenosine Triphosphatase pump type 1; HHD, Hailey–Hailey disease.

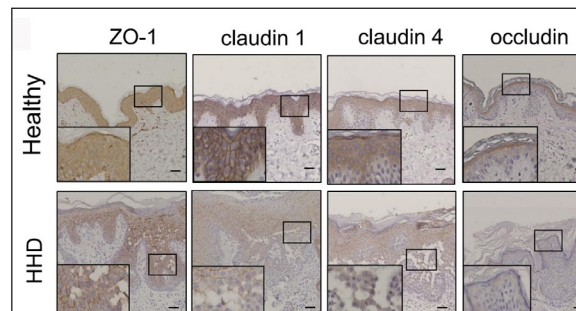


Figure 1b: SPCA1, cytoskeletal, and tight junction proteins are poorly expressed in the skin lesions of patients with HHD. Immunohistochemistry (IHC) was performed for the protein expression in the paraffin sections. HHD, Hailey–Hailey disease; ZO-1, zonula occludens protein 1.

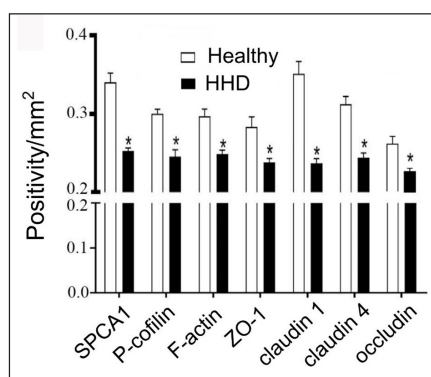


Figure 1c: SPCA1, cytoskeletal, and tight junction proteins are poorly expressed in the skin lesions of patients with HHD. ImageJ and GraphPad Prism 8.0 software determined the intensities of protein expressions. Scale bar = 50 μ m. * $p < 0.05$, compared to the healthy donors. SPCA1, Secretory pathway Ca^{2+}/Mn^{2+} Adenosine Triphosphatase pump type 1; HHD, Hailey–Hailey disease; ZO-1, zonula occludens protein 1.

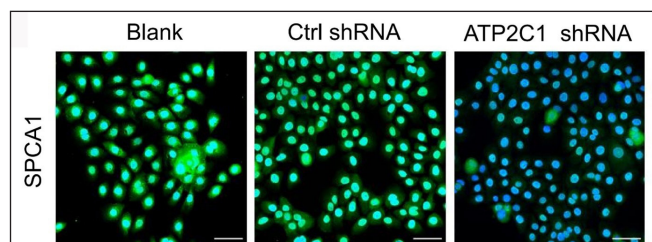


Figure 2a: Successful transfection of *ATP2C1* shRNA in keratinocytes. Immunofluorescence was performed to detect the SPCA1 expression. *ATP2C1*, Adenosine Triphosphatase calcium-transporting type 2C member 1 gene; SPCA1, Secretory pathway Ca^{2+}/Mn^{2+} Adenosine Triphosphatase pump type 1.

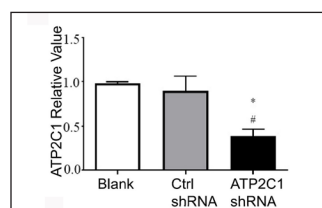


Figure 2b: Transfection of *ATP2C1* shRNA in keratinocytes. The mRNA expression of *ATP2C1* was determined in cells. * $p < 0.05$, compared to the blank groups; # $p < 0.05$, compared to the control shRNA group. *ATP2C1*, Adenosine Triphosphatase calcium-transporting type 2C member 1 gene.

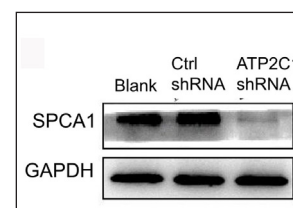


Figure 2c: Successful transfection of *ATP2C1* shRNA in keratinocytes. The expression of SPCA1 was analysed by Western blotting technique. *ATP2C1*, Adenosine Triphosphatase calcium-transporting type 2C member 1 gene; SPCA1, Secretory pathway Ca^{2+}/Mn^{2+} Adenosine Triphosphatase pump type 1; GAPDH, glyceraldehyde-3-phosphate dehydrogenase.

The levels of tight junction proteins decreased after *ATP2C1* knockdown

We detected the levels of claudin 1, claudin 4, occludin, and ZO-1 by immunofluorescence and simultaneously performed F-actin co-staining. The fluorescent intensities of F-actin and the four tight junction proteins in the *ATP2C1* shRNA group were significantly lower ($p < 0.05$), and no significant difference was observed between the two control groups [Figures 4a and 4b].

Further, we analysed the mRNA and protein levels of the tight junction proteins. The mRNA levels of claudin 1, claudin 4, occludin, and ZO-1 in the *ATP2C1* shRNA group decreased significantly compared with those in the two control groups ($p < 0.05$). [Figure 4c]. The western blotting technique results showed that the levels of the four tight junction proteins were lower in the *ATP2C1* shRNA group ($p < 0.05$), and no significant differences were observed between the two control groups [Figures 4d and 4e].

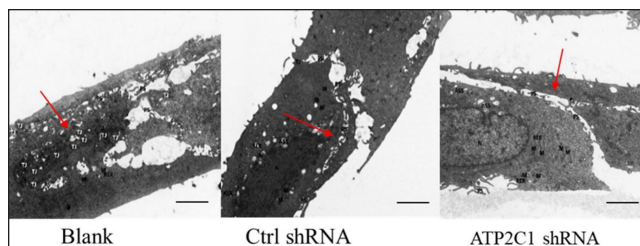


Figure 2d: Successful transfection of *ATP2C1* shRNA in keratinocytes. Electron microscopic structure of keratinocytes after *ATP2C1* gene knockout. Red arrows represent intercellular space. Scale bar = 2.5 μ m. *ATP2C1*: Adenosine Triphosphatase calcium-transporting type 2C member 1 gene.

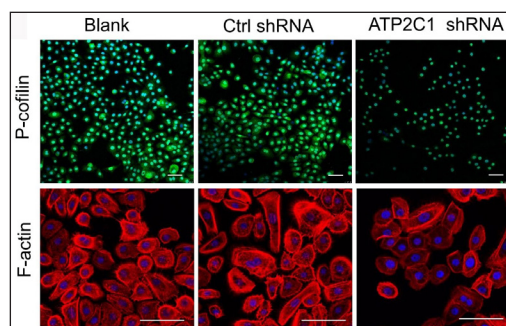


Figure 3a: The expressions of P-cofilin and F-actin are reduced after shRNA transfection in keratinocytes. Immunofluorescence was performed for the P-cofilin and F-actin expression. *ATP2C1*, Adenosine Triphosphatase calcium-transporting type 2C member 1 gene. Scale bar = 20 μ m.

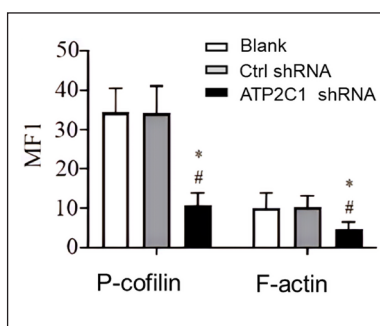


Figure 3b: The expressions of P-cofilin and F-actin are reduced after shRNA transfection in keratinocytes. The fluorescence intensities were quantitated by using the ImageJ and GraphPad Prism 8.0 software. *ATP2C1*, Adenosine Triphosphatase calcium-transporting type 2C member 1 gene. * $p < 0.05$, compared to the blank groups; # $p < 0.05$, compared to the control shRNA group.

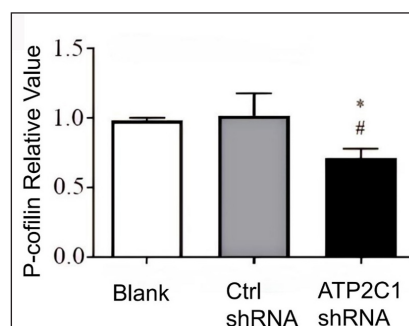


Figure 3c: The expressions of P-cofilin and F-actin are reduced after shRNA transfection in keratinocytes. The mRNA levels of P-cofilin in the cells were assessed after shRNA transfection. * $p < 0.05$, compared to the blank groups; # $p < 0.05$, compared to the control shRNA group. *ATP2C1*, Adenosine Triphosphatase calcium-transporting type 2C member 1 gene.

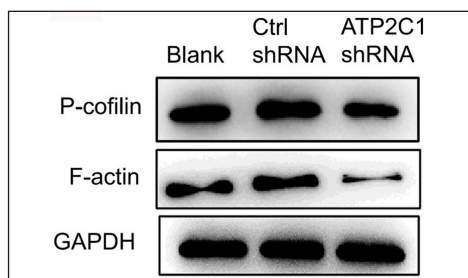


Figure 3d: The expressions of P-cofilin and F-actin are reduced after shRNA transfection in keratinocytes. The protein expressions were detected by Western blotting technique. GAPDH, glyceraldehyde-3-phosphate dehydrogenase; *ATP2C1*, Adenosine Triphosphatase calcium-transporting type 2C member 1 gene.

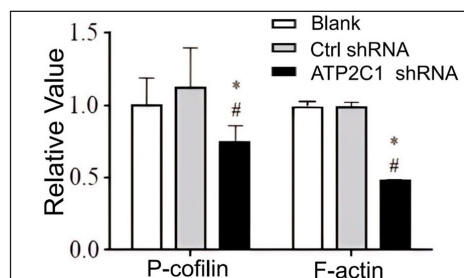


Figure 3e: Proteins of P-cofilin and F-actin were reduced after shRNA transfection in keratinocytes. The ImageJ software measured the band intensities. Data were from three independent experiments. *ATP2C1*, Adenosine Triphosphatase calcium-transporting type 2C member 1 gene. * $p < 0.05$, compared to the blank group; # $p < 0.05$, compared to the control shRNA group.

Cell apoptosis and intracellular Ca²⁺ influx were not affected by *ATP2C1* knockdown

The flow cytometry results showed that apoptosis ratios were similar between the three groups [Figures 5a and 5b]. The CCK-8 analysis showed that cell proliferation in the *ATP2C1* shRNA group was not altered [Figure 5c]. We detected intracellular Ca²⁺ concentrations in the keratinocytes using fluorescent microplates. However, no difference was observed in intracellular Ca²⁺ concentrations among the three groups [Figure 5d].

Discussion

The present study showed the dysregulation of cytoskeletal and tight junction proteins in HHD skin lesions. Moreover, a stable *in vitro* cell model of epidermal acantholysis with *ATP2C1* knockdown was successfully established in human keratinocytes. The levels of the cytoskeletal and tight junction proteins decreased because of a decrease in SPCA1 expression. Furthermore, cell apoptosis and proliferation, as well as intracellular Ca²⁺ influx, remained unaffected after *ATP2C1* knockdown.

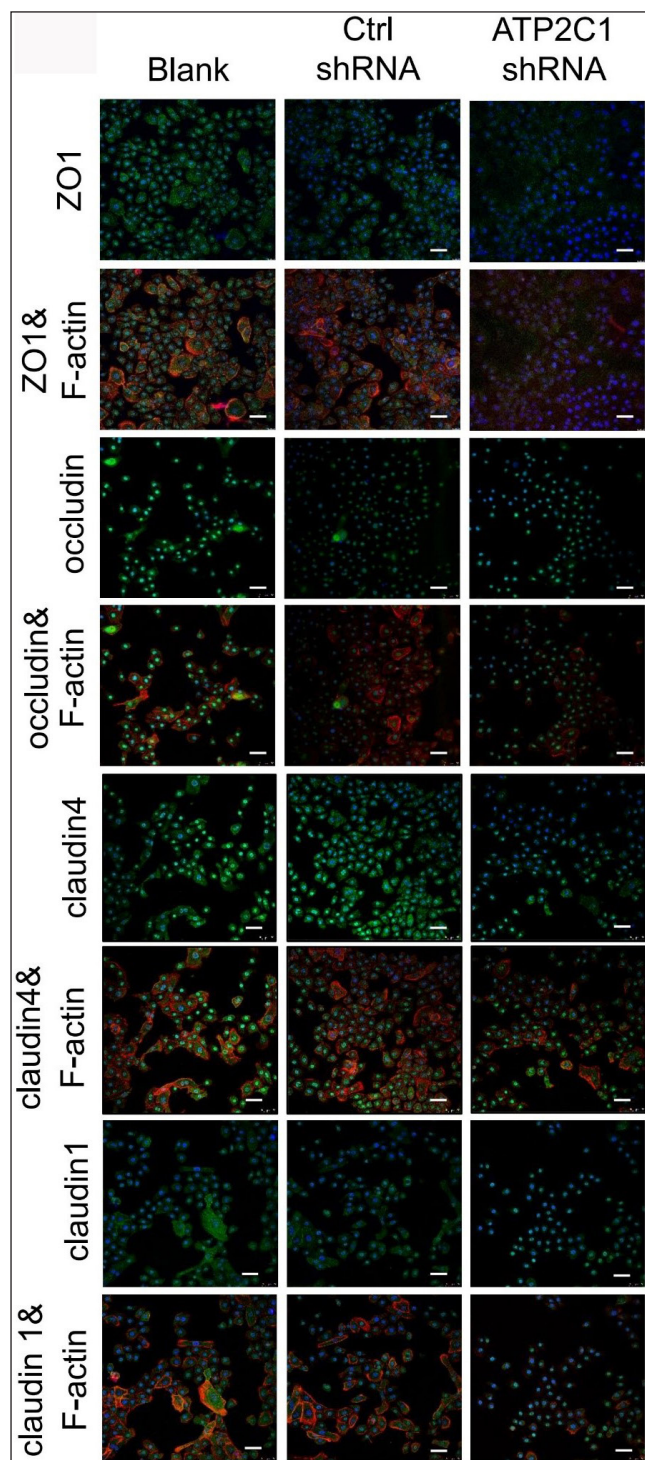


Figure 4a: The expressions of tight junction proteins after shRNA transfection in keratinocytes. Immunofluorescence was performed to detect the expression of tight junction proteins in the cells. *ATP2C1*, Adenosine Triphosphatase calcium-transporting type 2C member 1 gene; ZO-1, zonula occludens protein 1. Scale bar = 50 μm.

A study showed that SPCA1 stabilises the actin cytoskeleton by interacting with cofilin, which is bound to the phosphorylated region of SPCA1 in HeLa cells.⁷ *ATP2C1* controlled mouse neural tube closure by regulating cytoskeletal dynamics.¹² *ATP2C1* deficiency increased claudin and occludin levels in

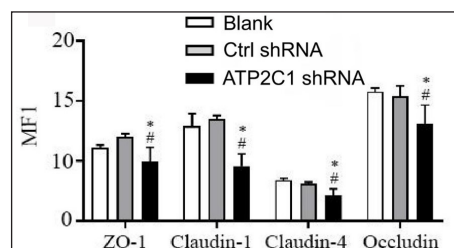


Figure 4b: The expressions of tight junction proteins after shRNA transfection in keratinocytes. ImageJ and GraphPad Prism 8.0 software quantified the fluorescence intensity of the tight junction proteins. * $p < 0.05$, compared to the blank groups; # $p < 0.05$, compared to the control shRNA group. *ATP2C1*, Adenosine Triphosphatase calcium-transporting type 2C member 1 gene; ZO-1, zonula occludens protein 1.

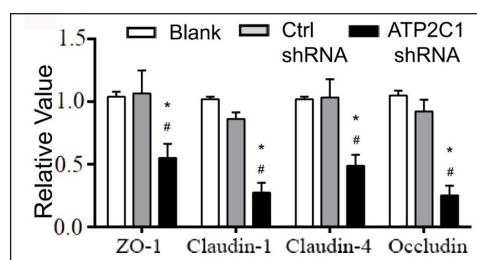


Figure 4c: The mRNA levels of tight junction proteins after shRNA transfection in keratinocytes. *ATP2C1*, Adenosine Triphosphatase calcium-transporting type 2C member 1 gene; ZO-1, zonula occludens protein 1. * $p < 0.05$, compared to the blank groups; # $p < 0.05$, compared to the control shRNA group.

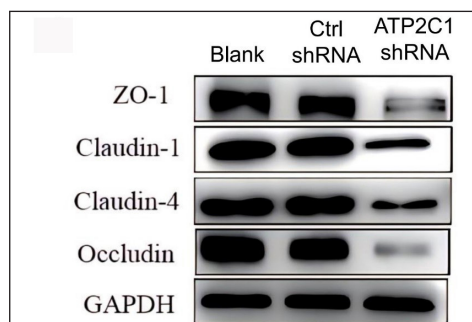


Figure 4d: The protein levels of tight junction proteins in keratinocytes were determined by Western blotting technique following shRNA transfection. *ATP2C1*, Adenosine Triphosphatase calcium-transporting type 2C member 1 gene; GAPDH, glyceraldehyde-3-phosphate dehydrogenase; ZO-1, zonula occludens protein 1.

keratinocytes and decreased ZO-1 levels.⁴ We examined the tight junction proteins in the lesion tissues and keratinocytes (*in vitro* model). SPCA1 maintains a balance between the levels of cytoskeletal and tight junction proteins,⁴ and the present findings are consistent with this observation. Conversely, the present study showed that P-cofilin and F-actin levels decreased in the skin lesions of patients with HHD. Moreover, their levels also fell in the cultured keratinocytes after a decrease in SPCA1 expression. Thus,

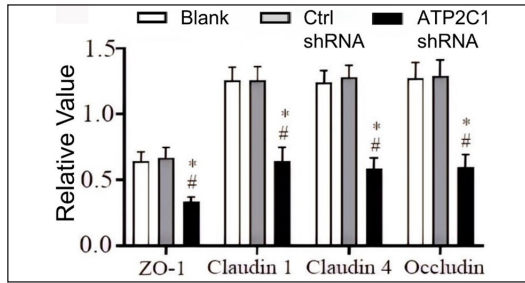


Figure 4e: The protein levels of tight junction proteins in keratinocytes were determined by Western blotting technique following shRNA transfection. The ImageJ software measured the intensity of protein bands. Data were from three independent experiments. *ATP2C1*, Adenosine Triphosphatase calcium-transporting type 2C member 1 gene; ZO-1, zonula occludens protein 1. * $p < 0.05$, compared to the blank groups; # $p < 0.05$, compared to the control shRNA group.

these results support the function of SPCA1 in regulating structural proteins related to epidermal acantholysis.

Currently, no suitable HHD animal model explicitly targets *ATP2C1* mutations.^{13,14} Different cell models for acantholysis exhibit poor efficiency and low stability for gene downregulation.¹⁵ A yeast-based HHD model has limitations in mimicking *in vivo* conditions.¹⁶ Thus, to better simulate HHD, we performed shRNA lentiviral transfection in human primary keratinocytes. The results showed that both the mRNA level of *ATP2C1* and the protein level of SPCA1 decreased significantly in the shRNA-transfected keratinocytes, and this characteristic was maintained even after multiple passages. Thus, we could successfully establish a cell model of HHD-like acantholysis with higher and more stable transfection efficiencies.

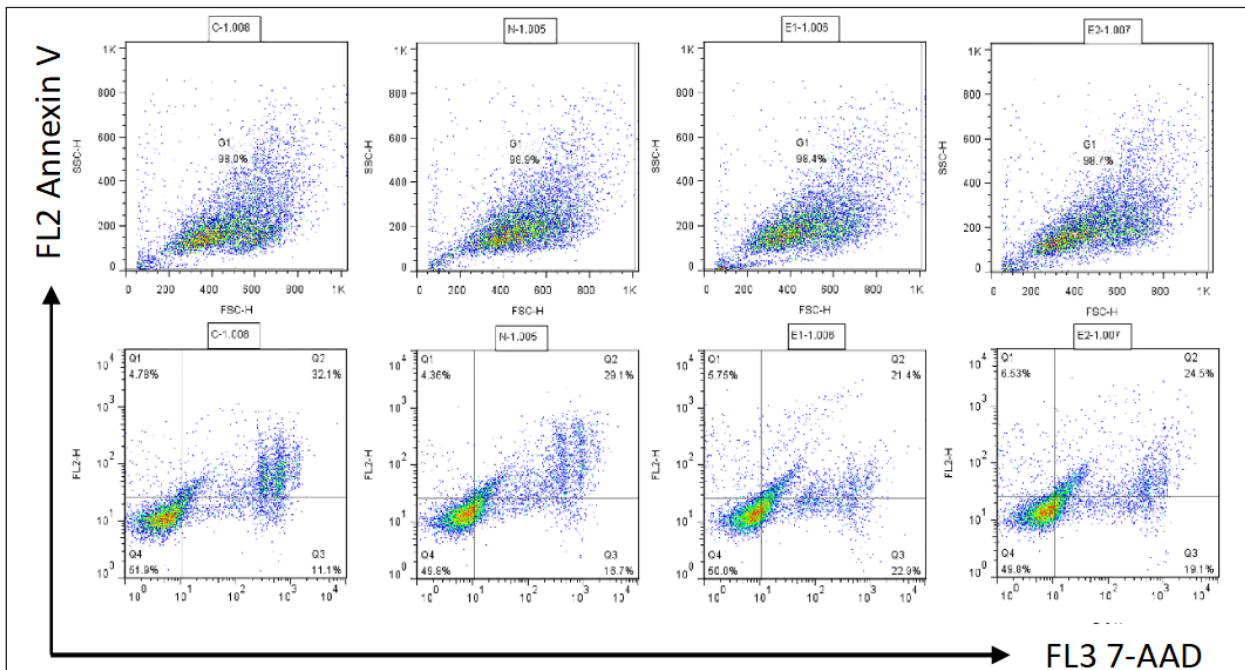


Figure 5a: The effect of *ATP2C1* gene knockdown on apoptosis was detected through flow cytometry. 7-ADD, 7-amino actinomycin D; Annexin V, annexin V-phycoerythrin; *ATP2C1*, Adenosine Triphosphatase calcium-transporting type 2C member 1 gene.

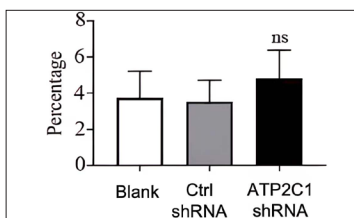


Figure 5b: The effect of *ATP2C1* gene knockdown on apoptosis was detected through flow cytometry. The ratios of apoptotic cells were quantified by ImageJ software. *ATP2C1*, Adenosine Triphosphatase calcium-transporting type 2C member 1 gene. ns, no statistical difference.

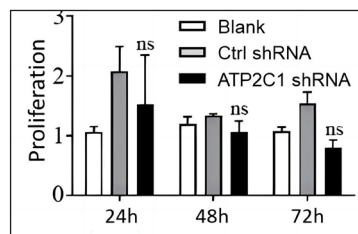


Figure 5c: The effect of *ATP2C1* gene knockdown on proliferation was measured by cell counting kit-8 (CCK-8). ns, no statistical difference. *ATP2C1*, Adenosine Triphosphatase calcium-transporting type 2C member 1 gene.

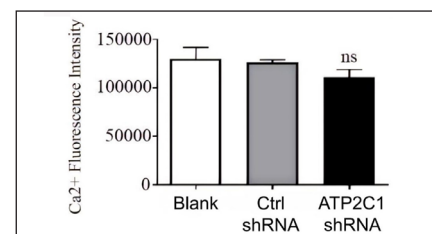


Figure 5d: The effect of *ATP2C1* gene knockdown on intracellular Ca²⁺ concentration was assessed using Fluo-3 Acetoxymethyl Ester (fluo-3 AM). ns, no statistical difference. *ATP2C1*, Adenosine Triphosphatase calcium-transporting type 2C member 1 gene.

Cofilin binds to SPCA1 at the trans-Golgi network to recruit F-actin and results in Ca²⁺ pump activation, thereby inducing Ca²⁺ influx into a specific domain of the trans-Golgi network.¹⁷ Epithelial cells use accumulated Ca²⁺ and F-actin to participate in cell adhesion and tight junction connections.¹⁸ Herein, we observed decreased levels of P-cofilin in the HHD cell model. The immunofluorescence results revealed a significant reduction in the fluorescence intensities of F-actin and P-cofilin in the *ATP2C1*-knockdown cells. The western blotting results supported this finding. These results showed that decreased P-cofilin levels caused the abnormal distribution of F-actin, suggesting its crucial role in HHD pathogenesis.

A study showed that the levels of tight junction proteins differed in keratinocytes cultured with different concentrations of Ca²⁺.⁴ Considering the effect of *ATP2C1* expression on the cellular Ca²⁺ concentration gradient,¹⁹ we examined intracellular Ca²⁺ concentrations. No difference was observed in intracellular Ca²⁺ concentrations among the three cell groups. This finding contrasted with Hu *et al.*'s study.²⁰ However, their study demonstrated that when two other calcium pumps were inhibited in keratinocytes cultured from patients with HHD, the cellular Ca²⁺ regulatory function significantly decreased. However, when the inhibition of the Na⁺/Ca²⁺ antiporter was reversed, the intracellular calcium concentration returned to normal, underscoring the pivotal role of Na⁺/Ca²⁺ antiporter in maintaining intracellular calcium levels. Furthermore, another study indicated that the Ca²⁺ concentration in keratinocytes derived from the skin of patients with HHD showed no difference compared with those derived from normal individuals, which aligns with our findings.^{21,22} Thus, we believe the intracellular Ca²⁺ concentration in keratinocytes that mimic HHD requires further investigation. The embryonic lethality observed in mice with *ATP2C1* mutations is probably associated with extensive cell apoptosis,¹³ and Ca²⁺ ions play a crucial role in mitochondrial apoptosis and cell apoptosis induction in HeLa cells.²² Thus, we examined keratinocyte proliferation and apoptosis after *ATP2C1* knockout. *ATP2C1* knockdown did not affect cell apoptosis and proliferation, suggesting that keratinocyte proliferation and apoptosis were unrelated to epidermal acantholysis in HHD.

Limitations

Our study was confined to cellular and tissue studies due to the unavailability of suitable animal models for HHD; thus, it may not ideally mimic the real *in vivo* environment. Given the rarity of HHD and the hesitancy of some patients to undergo skin biopsies, the number of patient samples acquired were comparatively limited. Additionally, we delved into the regulatory impact of *ATP2C1* inhibition on skeletal proteins and tight junction proteins, but our examination of their connection was somewhat constrained, and it awaits further study.

Conclusion

In summary, defects in *ATP2C1* play a pivotal role in HHD pathogenesis, and a decrease in SPCA1 expression in keratinocytes mimics multiple features of epidermal acantholysis. Thus, the present *in vitro* cell model may be used to explore treatment strategies for HHD. Moreover, a reduction in SPCA1 expression is associated with decreased P-cofilin and F-actin levels, thereby shedding light on the potential therapeutic targets for treating patients with HHD. Therefore, future studies should focus on the association between P-cofilin/F-actin and tight junction proteins in HHD.

Ethical approval

Furthermore, the research was approved by the Institute Ethical Committee of Xi'an Jiaotong University, with the assigned approval number 2016028.

Declaration of patient consent

The authors certify that they have obtained all appropriate patient consent.

Financial support and sponsorship

Nil.

Conflicts of interest

There are no conflicts of interest.

Use of artificial intelligence (AI)-assisted technology for manuscript preparation

The authors confirm that there was no use of artificial intelligence (AI)-assisted technology for assisting in the writing or editing of the manuscript, and no images were manipulated using AI.

References

- Roth-Carter QR, Burks HE, Ren Z, Koetsier JL, Tsoi LC, Harms PW, *et al.* Transcriptional profiling of rare acantholytic disorders suggests common mechanisms of pathogenesis. *JCI Insight* 2023:e168955.
- Zhang D, Xiao Z, Ouyang X, Wang X, Zhu Y, Yu S, *et al.* Two novel and a recurrent *ATP2C1* mutations in Chinese population with Hailey-Hailey disease. *Clin Cosmet Investig Dermatol* 2023;16:1545–8.
- Zhang D, Huo J, Li R, Zhang Y, Wang Z, Li X. Altered levels of focal adhesion and extracellular matrix-receptor interacting proteins were identified in Hailey-Hailey disease by quantitative iTRAQ proteome analysis. *J Cell Biochem* 2019;120:3801–12.
- Raiko L, Siljamaki E, Mahoney MG, Putaala H, Suominen E, Peltonen J, *et al.* Hailey-Hailey disease and tight junctions: Claudins 1 and 4 are regulated by the *ATP2C1* gene encoding Ca(2+)/Mn(2+) ATPase SPCA1 in cultured keratinocytes. *Exp Dermatol* 2012;21:586–91.
- Umeda K, Ikenouchi J, Katahira-Tayama S, Furuse K, Sasaki H, Nakayama M, *et al.* ZO-1 and ZO-2 independently determine where claudins are polymerized in tight-junction strand formation. *Cell* 2006;126:741–54.
- Schneeberger EE, Lynch RD. The tight junction: A multifunctional complex. *Am J Physiol Cell Physiol* 2004;286:C1213–28.
- Kienzle C, Basnet N, Crevenna AH, Beck G, Habermann B, Mizuno N, *et al.* Cofilin recruits F-actin to SPCA1 and promotes Ca²⁺-mediated secretory cargo sorting. *J Cell Biol* 2014;206:635–54.
- Li X, Zhang D, Ding J, Li L, Wang Z. Identification of *ATP2C1* mutations in the patients of Hailey-Hailey disease. *BMC Med Genet* 2020;21:120.

9. Liu W, Zhang D, Luo M, Jia F, Peng L, Li X, *et al.* TNF-like weak inducer of apoptosis promotes angiogenesis, thereby exacerbating cutaneous psoriatic disease. *J Invest Dermatol* 2021;141:1356–60.
10. Hu G, Liang L, Liu Y, Liu J, Tan X, Xu M, *et al.* TWEAK/Fn14 interaction confers aggressive properties to cutaneous squamous cell carcinoma. *J Invest Dermatol* 2019;139:796–806.
11. Sharma U, Singh SK, Rajendra P. Inverse correlation of intracellular calcium and cyclic AMP levels in renal cell carcinoma. *Cell Biochem Funct* 2012;30:619–22.
12. Brown JM, Garcia-García MJ. Secretory pathway calcium ATPase 1 (SPCA1) controls mouse neural tube closure by regulating cytoskeletal dynamics. *Development* 2018;145:dev170019.
13. Okunade GW, Miller ML, Azhar M, Andringa A, Sanford LP, Doetschman T, *et al.* Loss of the Atp2c1 secretory pathway Ca(2+)-ATPase (SPCA1) in mice causes Golgi stress, apoptosis, and midgestational death in homozygous embryos and squamous cell tumors in adult heterozygotes. *J Biol Chem* 2007;282:26517–27.
14. von Felbert V, Hampl M, Talhari C, Engers R, Megahed M. Squamous cell carcinoma arising from a localized vulval lesion of Hailey-Hailey disease after tacrolimus therapy. *Am J Obstet Gynecol* 2010; 203:e5–7.
15. Btadini W, Abou Hassan OK, Saadeh D, Abbas O, Ballout F, Kibbi AG, *et al.* Identification of several mutations in ATP2C1 in Lebanese families: Insight into the pathogenesis of Hailey-Hailey disease. *PLoS One* 2015;10:e0115530.
16. Voisset C, Garcia-Rodriguez N, Birkmire A, Blondel M, Wellinger RE. Using yeast to model calcium-related diseases: Example of the Hailey-Hailey disease. *Biochim Biophys Acta* 2014;1843:2315–21.
17. Pakdel M, von Blume J. Exploring new routes for secretory protein export from the trans-Golgi network. *Mol Biol Cell* 2018;29:235–40.
18. Vasioukhin V, Bauer C, Yin M, Fuchs E. Directed actin polymerization is the driving force for epithelial cell-cell adhesion. *Cell* 2000;100:209–19.
19. Yang L, Zhang Q, Zhang S, Liu Y, Liu Y, Wang T. Generalized Hailey-Hailey disease: Novel splice-site mutations of ATP2C1 gene in Chinese population and a literature review. *Mol Genet Genomic Med* 2020;9:e1580–e1594.
20. Hu Z, Bonifas JM, Beech J, Bench G, Shigihara T, Ogawa H, *et al.* Mutations in ATP2C1, encoding a calcium pump, cause Hailey-Hailey disease. *Nat Genet* 2000;24:61–5.
21. Leinonen PT, Myllylä RM, Hägg PM, Tuukkanen J, Koivunen J, Peltonen S, *et al.* Keratinocytes cultured from patients with Hailey-Hailey disease and Darier disease display distinct patterns of calcium regulation. *Br J Dermatol* 2005;153:113–7.
22. Boczek T, Sobolczyk M, Mackiewicz J, Lisek M, Ferenc B, Guo F, *et al.* Crosstalk among calcium ATPases: PMCA, SERCA and SPCA in mental diseases. *Int J Mol Sci* 2021;22:2785–808.